Title: Investigation the biomass conversion efficiency, biochemical characterisation and structural insights of the newly isolated AA16 family of Lytic Polysaccharide Monooxygenase (LPMO) from *Aspergillus fumigatus*.

Musaddique Hossain[1], Subba Reddy Dodda[1], Bishwajit Singh Kapoor[2], Kaustav Aikat[3] and Sudit S. Mukhopadhyay[1]*

Department of Biotechnology, National Institute of Technology Durgapur-713209, West Bengal, India

*Corresponding author: suditmukhopadhy@yahoo.com

Abstract

Efficient conversion of lignocellulosic biomass into fermentable sugar is a bottleneck for cheap production of bio-ethanol. Recently identified enzyme Lytic Polysaccharide Monooxygenase (LPMO) family has brought new hope because of its boosting capabilities of cellulose hydrolysis. Cellulase enzymes of *Aspergillus* origin are important for their thermo-stable nature. Here we have identified and characterized a new class of auxiliary (AA16) oxidative enzyme LPMO from the genome of a locally isolated thermophilic fungus *Aspergillus fumigatus* (NITDGPKA3). The biochemical, structural, and biomass conversion efficiency of *Af*LPMO16 have been explored. The *Af*LPMO16 is an intronless gene and encodes the protein of about 29kDa of molecular weight. Sequence-wise it is close to C1 type and structurally it is similar to AA11 family of LPMOs. The structure exclusively consists of loops and sheets. The gene was expressed under inducible promoter (AOX1) with C-terminal His tag in the *Pichia pastoris*. The protein was purified, and enzyme kinetics was studied with 2, 6-DMP. Polysaccharides hydrolysis activity was observed with Carboxymethyl cellulose (CMC) and Phosphoric acid swollen cellulose (PASC). Further, the lignocellulosic biomass conversion enhancement with Cellulase cocktail gives 2-fold enhancement in reducing sugar release suggests the importance of *Af*LPMO16 in the bio-ethanol industry.

Keywords: *A.fumigatus*, LPMO, cloning, kinetics, Molecular docking, lignocelluloses, Auxiliary activity

Introduction

The diminution of fossil fuels and the growing concern of environmental consequences particularly climate changes have steered our fast-growing economy towards the production of clean and renewable energy (DIAS DE OLIVEIRA et al. 2006). Among different renewable energy sources, bioethanol is one of the promising alternatives of fossil fuel, because of low CO_2 emission (Saricks et al. 1999; X. Lang, D. G. MacDonald, G. A. Hil 2002), and its manufacturing reliance on lignocellulosic biomass which is bio-renewable and abundance on earth. However, the structural complexity and the recalcitrance of this renewable carbon source (Somerville et al. 2004) has hindered its optimal use. The current process of saccharification of lignocellulosic biomass is time-consuming and costly. Therefore, the requirement of cost-effective and fast controlled destruction of lignocellulose has driven the bioethanol industry to explore the accessory enzymes to achieve a better and efficient enzyme cocktail for the commercial production of lignocellulose-derived ethanol.

A breakthrough on such exploration came into existence when a mono-copper redox enzyme, known as Lytic polysaccharide monooxygenase (LPMO) was unearthed in 2010 (Vaaje-Kolstad et al. 2010; Phillips et al. 2011; Quinlan et al. 2011; Johansen 2016). LPMO increases lignocellulosic biomass conversion efficiency (Harris et al. 2010; Müller et al. 2015) by catalyzing the hydroxylation of C1 and/or C4 carbon involved in glycosidic bonds that connect glucose unit in cellulose (Forsberg et al. 2011; Phillips et al. 2011; Quinlan et al. 2011). Therefore, allow Cellulase enzyme to further process the destabilised complex polysaccharides (Horn et al. 2012; Beeson et al. 2015; Vermaas et al. 2015). Harris et al. in their study showed that the degradation of polysaccharide substrates was increased by a factor of two when LPMO from *T reesei* was used with classical Cellulases (Harris et al. 2014). A CMB33 domain containing enzyme was identified from *Serratia marcescens* with boosting chitinase activity, later classified as LPMO (Forsberg et al. 2011). A study by Nakagawa et al. showed that an AA10 family of LPMO from *Streptomyces griseus* has the ability to increase the efficiency of chitinase enzymes by 30- and 20-fold on both α and β forms of chitin, respectively (Nakagawa et al. 2015). Along with these work, there are some recent reports of the synergisitc effect of LPMOs with glycoside hydrolases on polysaccharide substrates (Crouch et al. 2016; Chabbert et al. 2017; Liu et al. 2018b).

LPMOs were classified as AA9, AA10, AA11, AA13, AA14 and AA15 in CAZy database based on their amino acid sequence similarities until recent, when Filiatrault-Chastel et al. identified the AA16, a new family of LPMO from the secretome of a fungi *Aspergillus*

aculeatus (*Aa*AA16). The *Aa*AA16 was initially isolated as X273 protein (unnamed domain) and later identified as C1-oxidizing LPMO active on cellulose (Filiatrault-Chastel et al. 2019). Though it has some structural similarity with AA10, still, it possesses sufficient sequence dissimilarity with AA10 LPMOs. *Aa*AA16, the only AA16 family of LPMO so far has been identified and is very poorly understood. The biochemical characterization, structural characterization and moreover the assessment of biomass conversion efficiency are required to better understand the action of members of this new family on plant biomass and their possible biological roles.

While we were analyzing the cellulose hydrolyzing genes from the genome of of *A fumigatus* (*A fumigatus* genome database), five LPMOs have been identified and one of them was AA16 family which contains X273 domain. Later the *Af*LPMO16 gene was cloned from the genome of our locally isolated strain of *A fumigatus* (NITDGPKA3) (Sarkar and Aikat 2014) by designing the primer sequences based on the *A fumigatus* LPMO sequence (NCBI). The enzyme was characterized, three dimensional model structure was developed and assessment of the saccharification rate suggested that *Af*LPMO16 has fast and effective glucose releasing ability from lignocellulose and cellulose when it is used with commercial Cellulase coktail. Enzyme kinetics using 2,6-DMP as substrate (Breslmayr et al. 2018) confirmed the oxidative activity of the enzyme. So the biochemical and structural information and the efficiency in lignocellulosic biomass conversion suggested that *Af*LPMO16 could be an important member of the Cellulase cocktail of industrial use.

Materials and Methods

Sequence analysis and Phylogenetic analysis:

*Af*LPMO16 sequence (CAF32158.1) was obtained from NCBI and the sequence was further confirmed from the *Aspergillus* genome database (http://www.aspgd.org/). Homology sequence alignment was performed by the BLAST (Altschul et al. 1990). Clustal Omega (Sievers and Higgins 2014) was used for multiple sequence alignment. The sequence alignment was edited with Espript for better visualization. Pymol (DeLano 2002) and MEGA7 (Kumar et al. 2016) were used to construct phylogenetic tree. Neighbour joining tree was constructed with 1000 bootstrap replications.

Cloning of *Af*LPMO16

For tough filamentous fungi (e.g., Aspergillus and Fusarium spp.), cellular material is often snap-frozen in liquid nitrogen and milled in a pestle and mortar followed by rapid overtaxing in solution with an appropriate lysis buffer. Genomic DNA was isolated from the fungal biomass by using the DNA extraction buffer (400mM Tris-HCl, 150mM NaCl, 0.5M EDTA, 1%SDS) and followed by Phenol, chloroform and isoamyl alcohol (25:24:1) extraction. The final pellet was washed with 70% alcohol, air dried, and dissolved in sterile water. *Af*LPMO16 gene was amplified by polymerase chain reaction (PCR) using primers (Forward 5'ca***GAATTC***ATGAAGCAAACCGGCACTCTCGTCGCCC 3' and Reverse 5'ct*G**CGGCCGCA***GCAATATACTGCAGCAGGCTCTTCAG 3') and cloned in *Eco*R1 and *Not*1 sites (restriction enzymes are shown in the bold and italic) of pPICZαA vector (Invitrogen). pPICZαA vector contains alpha-factor signal sequence for extracellular secretion. The gene was cloned into the pPICZαA vector such a way that the *Af*LPMO16 carries the both alpha-factor signal sequence and His tag at the C-terminal. The clone was transformed into DH5α cell of *E.coli* and further confirmed by sequencing (Supplementary data 1).

Expression and purification of *Af*LPMO16

The linearized positive clone of *Af*LPMO16 (pPICZαA-*Af*LPMO16) was transformed into *P. pastoris X33* genome. The positive colonies were selected on YPDS (Zeocin) plates. The positive colonies were further screened by the colony PCR and expression studies. Protein expression was carried out initially in BMGY media and then transferred into BMMY medium with continuous induction by addition of 1% methanol (optimized) every day for three days. After three days the culture media was spun down (8,000rpm for 10mins) at 4^0C. The pellet was discarded and the media was collected. As the protein contains the C-terminal secretary sequence, the protein was precipitated from the media by Ammonium sulphate precipitation (100% saturation). The recombinant protein was purified by immobilized ion affinity chromatography (Ni-NTA affinity chromatography) (Bennati-granier et al. 2015) followed by dialysis with 50mM phosphate buffer, pH- 5.8. The yield of the purified protein was almost 0.8 mg/ml. The concentration was measured by Bradford assay, and BSA was used for standard concentration. The protein was separated by 12% SDS-PAGE, stained with coomassie blue and the protein band was also confirmed by Western blot analysis by using His-antibody (Abcam).

Biochemical assays of *Af*LPMO16

2,6 DMP (2,6-dimethoxyphenol) was used as a substrate for *Af*LPMO16 in this study (Breslmayr et al. 2018). The reaction was done in phosphate buffer (100mM pH 6.0) containing 10mM DMP, 5µM hydrogen peroxide, and 50µg of purified *Af*LPMO16 at 30℃. The amount of product 1-coerulignone was measured by spectrophotometer using the standard extinction coefficient (53200$M^{-1}cm^{-1}$) and Lambert-beer law. For kinetic assay different DMP concentrations (1mM,5 mM,10 mM,20 mM,25mM, 30mM, 40mM, 50mM, 70mM, 100mM) were used. The kinetic parameters were calculated based on Line-weaver-Burk plot. One unit of enzyme activity defined as the amount of enzyme which releases 1µM of 1-coerulignone (product) per minute in standard condition.

Different cellulosic compounds such as PASC, avicel®PH-101 (SIGMA) and carboxyl methylcellulose (CMC) were used. We used 1% avicel®PH-101 (SIGMA) (crystalline cellulose) and 1% CMC (Carboxyl methyl cellulose sodium salt) with different concentrations of purified *Af*LPMO16 for different time period incubation. Reducing sugar was determined by Dinitro salicylic acid (DNS) assay. For PASC assay we used 0.25% PASC and incubated with increasing concentration of *Af*LPMO16 for 6 hours and measured the OD after 6hrs of incubation and plot the relative absorbance ([OD of *Af*LPMO16 treated PASC]-[OD of untreated substrate]) with enzyme concentration (Hansson et al. 2017).

Both cellulose and lignocellulose (alkaline pre-treated raw rice straw) (Yoswathana 2010) were used for determining the cellulose hydrolysis enhancing capacity. Rice straw was pre-treated with 5% NaOH (1:10 W/V ratio) at 120℃ at 15Psi pressure for 1 hour and sodium azide (20%) 10µl (per 10ml) was added at the reaction mixture to prevent any microbial contamination. The reaction was performed at 50℃ and the amount of reducing sugar was estimated after 5hours, 24hours, 48hours, and 72 hours by Dinitro salicylic acid (DNS) assay. 20µl of cellulase (MP Biomedicals LLC) (5mg/ml) was used along with two different concentrations of *Af*LPMO16 (100µg and 200µg). *Af*LPMO16 was heat inactivated by keeping at 100℃ temperature for 30 minutes. In case of cellulose degradation, 400µl (1%) of avicel (SIGMA) was incubated with 10µl of cellulase (MP Biomedicals LLC) (5mg/ml). Reducing sugar was estimated after 5 hours of incubation. For these biochemical assays we used 100mM phosphate buffer (pH-6.0) and heat inactivated *Af*LPMO16 was taken as negative control.

Molecular modelling and Molecular docking

I-TASSER (Zhang 2008) server was used to model the *Af*LPMO16. The final model was energy minimized by Gromacs software (Pronk et al. 2013). The final model was evaluated by the Ramachandran plot (Gopalakrishnan et al. 2007) and Procheck (Laskowski et al. 2002). The Metal Ion-Binding site prediction and docking server or MIB server (http://bioinfo.cmu.edu.tw/MIB/) was used to identify the copper (Cu) ion position. Molecular docking study was performed by the Autodock Vina (Trott and Olson 2010) using MGL tools. The optimized substrate structures were prepared by Autodock vina and saved in pdbqt format. The grid size parameters used in this docking were 44, 46, 46 and grid centre parameters used in this study were 49, 45 and 55. The genetic algorithm was also used for docking. Molecular interactions between enzyme and substrate was analyzed by the MGL tools (Morris et al. 2009).

Results

In silico analysis of *Af*LPMO16

The *Af*LPMO16 contains N terminal signal peptide (1-19aa), Catalytic domain (20-189aa) and C terminal Serine rich region (190-290aa) (Fig. 1a) but CBM1 module or a glycosylphosphatidylinositol (GPI) anchor is absent like some other AA16 LPMOs (Filiatrault-Chastel et al. 2019). *Af*LPMO16 also has conserved histidine at 20 and 109 positions, which are mainly involved in copper binding. There are other conserved sequences like Gly, Pro, Asn, Cys, Try, Tyr, Leu, and Asp including GN (Y)V(T)QGELQ motif (Fig. 1b & 1c). In Chitin active LPMOs, more than 70% residues of the motif (Y (W) EPQSVE) are polar including two are negatively charged Glu (E). In Cellulose active LPMOs, 70% residues of the motif (Y (W) NWFGVL) are hydrophobic. In contrast, in *Af*LPMO16, 70% residues are polar including one negatively charged Glu (E), one hydrophobic Tyr (Y), and others are neutral. The presence of polar residue and negative charged Glu (E) suggests that *Af*LPMO16 may bind to chitin. Electrostatics interaction between the substrate and enzyme active site plays a pivotal role in substrate binding. Electrostatic potential surface at the catalytic site of the *Af*LPMO16 was found unchanged or slightly positive charged at pH 6.0 (Fig. 1D) (Marked in the figure). The electrostatic interaction study suggests that the *Af*LPMO16 may also bind to cellulose (Pantoom et al. 2008). So in-silico analyses suggest that the *Af*LPMO16 has some signature characteristics for both cellulose and chitin binding.

Amino acids on substrate binding surface determine the oxidative regioselectivity of LPMOs (Zhou and Zhu 2020). Sequence comparison and mutation studies revealed that the conserved

amino acids near catalytic center in C1 and C1/C4 oxidizing AA10 and AA9 LPMOs are responsible for regioselectivity. In case of C1/C4 oxidizing AA10 the amino acid Asn85 near catalytic center is responsible for C4 oxidising activity. Alteration of this amino acid (N85F) diminished the C4 activity and produced only C1 oxidized product (Forsberg et al. 2014). In C1 oxidizing AA9 LPMOs, hydrophobic amino acids Phe and Tyr are conserved in addition to Asn. While in C1 oxidizing AA10 LPMOs, the corresponding Asn site is replaced by Phe amino acid (Fig. 1c). The Phe is also parallel to the substrate binding surface (Liu et al. 2018a). In AA16 the corresponding Gln (Q) is parallel to the substrate-binding region (Fig. 1c). The function of conserved Gln (Q) is not clear. But this polar amino acid is having similar side chain with polar Asn (N). The axial distance between conserved amino acid and copper catalytic center is another important factor for regioselectivity. The C1/C4 oxidising AA10 LPMOs have more open or wider axial distance compare to C1 oxidizing AA10 LPMOs (Forsberg et al. 2014). Here the distance between Gln56 and His20 is 7.7Å and the distance between Gln56 and Cu catalytic center is 11.1Å. In absence of AA16 structure (crystal or model) we cannot compare the distances. But this distance may play a key role in regioselectivity. This sequence-based analysis is speculative and needs further experimental confirmation. So the *Af*LPMO16 might have both C1 and C4 oxidizing capability in spite of having more sequence similarity with C1 oxidizing LPMOs.

Based on sequence comparison, *Af*LPMO16 is evolutionary more close to the LPMO of *Aspergillus fisheri* (91% sequence homology). The constructed phylogenetic tree contains two main clades and two sub clades (Fig. 1e). The first clade contains all AA10 LPMOs from bacterial species such as *Bacillus thuringiensis*, *Bacillus amyloliquefaciens, Streptomyces lividans,* and *Enterococcus nsnfaecails*. The second clade contains all fungal AA10, AA16 LPMOs, mainly belongs to *Aspergillus,* and *Penicillium* species in which AA16 LPMOs are mostly from *A.niger*, *A.fumigatus*, *A.fisheri*, *Aspergillus skawachi* (Fig. 1e).

Modeling and molecular docking analysis

The three dimensional structure of the *Af*LPMO16 is predicted by the I-TASSER. Most of the LPMOs have immunoglobulin like distorted β-sandwhich fold like structures, in which antiparallel 7 β-strands are connected by loops with different number of α-helix insertions (Fig. 2a). The final model has β-sandwhich structure connected by loops with two α-helices. The super imposition of the *Af*LPMO16 with other LPMO families like AA9, AA10, AA11, and AA13 showed that they share common antiparallel β-strands and helices with more

loops. Moreover *Af*LPMO16 showed 1.2Å RMSD with AA11 (PDB Id: 4MAH) LPMO, which is lower than the other LPMOs. So the 3D structure of *Af*LPMO16 suggests that it has more structural resemblance with AA11 LPMO. One disulfide bond was found in *Af*LPMO16 and it was formed by the Cys78-Cys186 amino acids (supplementary Fig. 3). The Cu ion is coordinated by the histidine brace amino acids such as His20 and His109. The active site was found on the surface of *Af*LPMO16 (Fig. 2b). The interaction studies with cellohexose suggested the amino acids like Gln48, Gln181, Ser178, His109, His20, Asn54, Asp50, Ty252, and Glu58 are in the active site and are involved in the interaction with the substrate (Fig. 2c).

Expression and purification of *Af*LPMO16

*Af*LPMO16 is an intronless gene having a length of 870 nucleotides and encodes 290 amino acids. The suggested molecular weight is 29KDa. The amino acid sequence of AA16 from our isolated strain of *A fumigatus* (NITDGPKA3) has shown almost 99.6% homology with the genome database of *A fumigatus* (CAF32158.1)(NCBI database) (Supplementary data 1). The expression was optimized and approximately 0.8 mg/ml purified protein was achieved by Ni-NTA affinity chromatography. The SDS-PAGE analysis (Fig 3a) is showing the purified protein bands (Fig. 3a; lane 5 and 6) which were further confirmed by Western blot analysis using anti-His antibody (Fig. 3b). The activity of the protein was also verified by using 2,6 DMP as substrate (Breslmayr et al. 2018). The expressed recombinant *Af*LPMO16 band appeared at approximately 32kDa position in SDS-PAGE (Fig. 3a), which is slightly higher than the expected size and probably due to glycosylation and other post translational modification (Bennati-granier et al. 2015).

Oxidative activity of *Af*LPMO16

LPMO converts 2, 6-dimethoxyphenol (2, 6-DMP) into 1-Coerulignone (Fig. 4a) due to its oxidative property and 1- Coerulignone has an extinction coefficient of 53200$M^{-1}cm^{-1}$. 1-Coerulignone gives absorbance at 469nm wavelength; therefore, it can easily be quantified using spectrophotometer (Breslmayr et al. 2018). Temperature and pH influence the activity of LPMO. Thus, during the kinetic study, we used optimum temperature 30℃ and pH 6.0 as described by *Breslmayr et al.*2018. *Af*LPMO16 showed proper activity for the chemical substrate 2,6-DMP (Fig. 4b), as, there was a steady release of 1-Coerulignone when incubated 2,6-DMP with *Af*AA16. In 150 seconds nearly 2.1µM product (1- Coerulignone) released (Fig. 4b). This result confirms the oxidative activity of the enzyme *Af*LPMO16. But

no product was observed with heat inactivated enzyme (data not shown). The calculated specific activity of *Af*AA16 was 37.43 U/g for the substrate 2, 6-DMP. The Kinetics parameters such as Michaelis Menten constant (K_m) and maximum velocity (V_{max}) were obtained from Line-weaver-Burk plot (Fig. 4c) and were found as 11.23µM, and 1.1086µM/min respectively. The calculated catalytic activity K_{cat} was 0.642 /min (Table 1). These kinetics parameters suggesting that the oxidative property of *Af*LPMO16 nearly same compared to other LPMOs.

Glycosidase activity of *Af*LPMO16

*Af*LPMO16 showed efficient glycosidase activity on both CMC and PASC (Fig. 5a & 5b) but insufficient activity (negligible amount of reducing sugar was produced) was found on cellulose (data not shown). The amount of reducing sugar released by enzymatic degradation was estimated. When CMC was incubated with increasing concentrations of enzyme the amount of product (reducing sugar) was also increased with the increasing of *Af*LPMO16 concentration (Fig. 5a). When 50µg of enzyme was added nearly about 0.05mg/ml of reducing sugar was released. For 100µg of enzyme the product was nearly 0.136mg/ml and for 200µg of enzyme the amount of product released was approximately 0.356mg/ml (Fig. 5a). This result clearly indicates the polysaccharide (CMC) depolymerization activity of *Af*LPMO16.

In another experiment we used insoluble PASC as a substrate and incubated with increasing concentration of *Af*LPMO16. The relative absorbance of PASC was determined with the increasing amount of enzyme. The enzyme degrades the polysaccharide (substrate) into smaller polysaccharide units (monosaccharides, disaccharides etc.), which are soluble and will lead to decrease the absorbance. Hence the relative absorbance with respect to untreated substrate has increased with the addition of high concentration of enzyme *Af*LPMO16 (Fig. 5b). The graph (Fig. 5b) showed that 0.17 absorbance difference with respect to untreated substrate when 50µl (concentration 0.8µg/µl) of enzyme was used. The difference in absorbance steadily increased with escalation of enzyme concentration (200µl of enzyme at the concentration of 0.8µg/µl the relative absorbance reached to nearly 0.36). Hence these experiments clearly confirmed the intrinsic glycosidase property of the *Af*LPMO16 like other LPMOs. In these experiments cellulase cocktail and heat inactivated *Af*LPMO16 was used to verify the authenticity of these results (data not shown).

Synergistic effect of *Af*LPMO16

The LPMOs are important for their auxiliary activity. It enhances the activity of Cellulase enzyme for degradation of cellulose and lignocelluloses (Corrêa et al. 2019). The only identified AA16 family, the *Aa*AA16 showed sequential synergistic effect with *T. reesei* CBHI on nano-fibrillated cellulose (NFC) and PASC. Here the synergistic effect of *Af*LPMO16 was studied with Cellulase cocktail on both cellulose (Avicel) and lignocellulose (alkaline pre treated rice straw). When Avicel was incubated with *Af*LPMO16 along with Cellulase the amount of reducing sugar released was almost double compared to Avicel incubated with only Cellulase and Cellulase along with heat inactivated *Af*LPMO16 (Fig. 6b). The similar kind of boosting effect was observed in every time points from 5 hrs to 72 hrs. The synergistic effect of *Af*LPMO16 was also observed in lignocellulosic biomass transformation (Fig. 6a). When the alkaline pre-treated rice straw was incubated with 100 µg and 200µg of *Af*LPMO16 along with cellulase almost 1.7 fold and slightly above than 2-fold of glucose were released respectively compared to lignoclellulose treated with only Cellulase and Cellulase along with heat inactivated *Af*LPMO16 (Fig. 6a). So this enhancement is dependent on the amount of auxiliary enzyme *Af*LPMO16. All these results confirmed the boosting effect or synergistic effect of *Af*LPMO16 on hydrolytic activity of cellulase for both cellulosic and lignocellulosic biomass degradation.

Discussion

From discovery to implementation in the bioethanol industry, the positive effect of LPMO is well demonstrated. LPMO has intrinsic oxidase and glycosidase properties. But more important is that it can enhance the biomass converion efficiency of the Cellulase. So far highest synergistic effect was reported by AA9 which is less than two fold (Zhang et al. 2019). *Aa*AA16, the recent addition of AA16 family of LPMO in the CAZY database showed synergism with CBH1 for the degradation of cellulose. But the detail biochemical characteristic is required to consider this family as an important member of the Cellulase cocktail for bioethanol industry. In this work we have characterized the *Af*LPMO16, which in our knowledge is the second member of the AA16 family. *Af*LPMO16 shares many common features like N-terminal signal peptide, catalytic domain and Serine-rich C-terminal domain (Fig.1a). It contains the conserved amino acids like copper binding Histidine (20 and 109) and GN (Y)V(T)QGELQ motif (Fig. 1b). In silico analysis and molecular docking suggest that *Af*LPMO16 has cellulose-binding surface, chitin-binding surface and serine-rich C

terminal domain for binding of lignin (Fig 2b, 2c & supplementary Fig 1). Based on the binding energy the binding between cellulose and *Af*LPMO16 is thermodynamically more stable than any other substrates (-7.0Kcal/mol). But experimental confirmation is required to establish its chitin and lignin binding nature. Similarly some marker motifs manifest the both C1 and C4 oxidizing mechanism for *Af*LPMO16 and experimental studies are required to confirm the C1 or C4 oxidizing properties of *Af*LPMO16. Our 3D model structure of *Af*LPMO16 (Fig. 2a) suggests the high percentage of loop compare to other LPMOs which indicates the high flexibility and thermo-stability of the enzyme. In lignocellulosic biomass hydrolysis assay, the retention of enzyme activity up to 72 hours at 50℃ (Fig. 6a) is also an indication of the thermo-stable nature of *Af*LPMO16. Here this is the first time we were able to characterize the AA16 family of enzyme biochemically. The activity assay based on 2,6-DMP detected the oxidative activity of *Af*LPMO16 (Fig. 4b). This spectrophotometric assay is very fast, robust and helps in screening, purification and production of the enzyme including enzyme kinetic study (Breslmayr et al. 2018). We were successful in producing the active *Af*LPMO16 in *P pastoris* and shake flask. Though it might have some chance of N-terminal modification in shake flask culture instead of bioreactor culture (Filiatrault-Chastel et al. 2019). But we got sufficient activity and enzyme activities were always checked with the heat inactivated enzyme. Hopefully the activity assay based on 2,6-DMP is very fast compared to MS/HPLC- based assay. MS/HPLC- based assays are time taking and enzyme may loose its activity within this time due to its auto oxidation (Dejan-Bastein et al. 2018). Glycosidase activity was observed on carboxymethyl cellulose (CMC) and phosphoric acid swollen cellulose (PASC) (Fig. 5a & 5b). But it didn't show sufficient activity on Avicel. This result indicates that the exo-glucanase activity of the *Af*LPMO16 is absent which is required for depolymerization of the crystalline structure of the Avicel (Väljamäe et al. 1999; Asztalos et al. 2012). This particular family of enzyme has earned so much research interest due to its synergistic effect or boosting effect on cellulase enzyme (Zhang et al. 2019). *Af*LPMO16 showed boosting effect on both cellulose and lignocellulose (Fig. 6 & 6b) which is higher than other LPMO families (Hu et al. 2018). But the mechanism of synergism with cellulase enzyme complex is poorly understood. Hopefully the cellulose biomass is partially depolymerized by the LPMO, which gives further access of the cellulase enzymes. The copper ion in the active site requires the presence of redox-active cofactor to potentiate the oxidation activity. The cofactors like hydrogen peroxide or Cellobiose dehydrogenase (CDH) have been reported (Tan et al. 2015). Though further study is required but the initial docking studies suggest that the association of Cellobiose dehydrogenase with *Af*LPMO16 is better

than hydrogen peroxide (supplementary Fig. 2).

In conclusion, the *Af*LPMO16 is the second report of AA16 family of LPMO but for the first time we have characterized the AA16 family biochemically and structurally. In-silico sequence analysis, structure analysis and molecular docking studies suggest some unique characteristics of the *Af*LPMO16 like cellulose, chitin, lignin binding ability and both C1 and C4 oxidizing property. Further studies are required to confirm these characteristics. But most important is the significant boosting effect on Cellulase cocktail in lignocellulosic biomass conversion and that suggests its importance in bioethanol industry.

Author contribution

MH and SM designed the research and wrote the manuscript. MH performed biochemical assays. SRD performed In-sillico analysis. MH, BSK and KA analyzed the results. All authors read and approved the manuscript.

Acknowledgements

This study is financially supported by the DBT, Govt. of India (Grant No. BT/PR13127/ PBD/26/447/2015). MH is thankful to DBT and SRD is thankful to DST Inspire for their fellowship. Authors are also thankful to DST-FIST grant of the Department of Biotechnology, NIT Durgapur.

Compliance with ethical standards

Conflict of interest Authors have no competing interest. Manuscript has been 'spell checked', 'grammar checked' and “plagiarism checked” by “Grammarly”.

Ethical approval No human participants or animal is being used during the study.

.

Reference:

Altschul SF, Gish W, Miller W, Myers EW, Lipman DJ (1990) Basic local alignment search tool. J Mol Biol. https://doi.org/10.1016/S0022-2836(05)80360-2

Asztalos A, Daniels M, Sethi A, Shen T, Langan P, Redondo A, Gnanakaran S (2012) A

coarse-grained model for synergistic action of multiple enzymes on cellulose. Biotechnol Biofuels. https://doi.org/10.1186/1754-6834-5-55

Beeson WT, Vu V V., Span EA, Phillips CM, Marletta MA (2015) Cellulose Degradation by Polysaccharide Monooxygenases. Annu Rev Biochem. https://doi.org/10.1146/annurev-biochem-060614-034439

Bennati-granier C, Garajova S, Champion C, Grisel S, Haon M, Zhou S, Fanuel M, Ropartz D, Gimbert I, Bennati-granier C, Garajova S, Champion C, Grisel S, Haon M, Bennati-granier C, Garajova S, Champion C, Grisel S, Haon M (2015) Substrate specificity and regioselectivity of fungal AA9 lytic polysaccharide monooxygenases secreted by Podospora anserina To cite this version : Substrate specificity and regioselectivity of fungal AA9 lytic polysaccharide monooxygenases secreted by Pod. Biotechnol Biofuels. https://doi.org/10.1186/s13068-015-0274-3

Breslmayr E, Hanžek M, Hanrahan A, Leitner C, Kittl R, Šantek B, Oostenbrink C, Ludwig R (2018) A fast and sensitive activity assay for lytic polysaccharide monooxygenase. Biotechnol Biofuels. https://doi.org/10.1186/s13068-018-1063-6

Chabbert B, Habrant A, Herbaut M, Foulon L, Aguié-Béghin V, Garajova S, Grisel S, Bennati-Granier C, Gimbert-Herpoël I, Jamme F, Réfrégiers M, Sandt C, Berrin JG, Paës G (2017) Action of lytic polysaccharide monooxygenase on plant tissue is governed by cellular type. Sci Rep. https://doi.org/10.1038/s41598-017-17938-2

Corrêa TLR, Júnior AT, Wolf LD, Buckeridge MS, Dos Santos LV, Murakami MT (2019) An actinobacteria lytic polysaccharide monooxygenase acts on both cellulose and xylan to boost biomass saccharification. Biotechnol Biofuels 12:1–14 . https://doi.org/10.1186/s13068-019-1449-0

Crouch LI, Labourel A, Walton PH, Davies GJ, Gilbert HJ (2016) The contribution of non-catalytic carbohydrate binding modules to the activity of lytic polysaccharide monooxygenases. J Biol Chem. https://doi.org/10.1074/jbc.M115.702365

DeLano W. . (2002) Pymol: An open-source molecular graphics tool. CCP4 Newsl Protein Crystallogr

DIAS DE OLIVEIRA ME, VAUGHAN BE, RYKIEL EJ (2006) Ethanol as Fuel: Energy, Carbon Dioxide Balances, and Ecological Footprint. Bioscience. https://doi.org/10.1641/0006-3568(2005)055[0593:eafecd]2.0.co;2

Filiatrault-Chastel C, Navarro D, Haon M, Grisel S, Herpoël-Gimbert I, Chevret D, Fanuel M, Henrissat B, Heiss-Blanquet S, Margeot A, Berrin JG (2019) AA16, a new lytic polysaccharide monooxygenase family identified in fungal secretomes. Biotechnol Biofuels. https://doi.org/10.1186/s13068-019-1394-y

Forsberg Z, Mackenzie AK, Sørlie M, Røhr ÅK, Helland R, Arvai AS, Vaaje-Kolstad G, Eijsink VGH (2014) Structural and functional characterization of a conserved pair of bacterial cellulose-oxidizing lytic polysaccharide monooxygenases. Proc Natl Acad Sci U S A. https://doi.org/10.1073/pnas.1402771111

Forsberg Z, Vaaje-kolstad G, Westereng B, Bunsæ AC, Stenstrøm Y, Mackenzie A, Sørlie M, Horn SJ, Eijsink VGH (2011) Cleavage of cellulose by a cbm33 protein. Protein Sci. https://doi.org/10.1002/pro.689

Gopalakrishnan K, Sowmiya G, Sheik SS, Sekar K (2007) Ramachandran plot on the web (2.0). Protein Pept Lett

Hansson H, Karkehabadi S, Mikkelsen N, Douglas NR, Kim S, Lam A, Kaper T, Kelemen B, Meier KK, Jones SM, Solomon EI, Sandgren M (2017) High-resolution structure of a lytic polysaccharide monooxygenase from Hypocrea jecorina reveals a predicted linker as an integral part of the catalytic domain. J Biol Chem 292:19099–19109 . https://doi.org/10.1074/jbc.M117.799767

Harris P V., Welner D, McFarland KC, Re E, Navarro Poulsen JC, Brown K, Salbo R, Ding H, Vlasenko E, Merino S, Xu F, Cherry J, Larsen S, Lo Leggio L (2010) Stimulation of

lignocellulosic biomass hydrolysis by proteins of glycoside hydrolase family 61: Structure and function of a large, enigmatic family. Biochemistry. https://doi.org/10.1021/bi100009p

Harris P V., Xu F, Kreel NE, Kang C, Fukuyama S (2014) New enzyme insights drive advances in commercial ethanol production. Curr. Opin. Chem. Biol.

Horn SJ, Vaaje-Kolstad G, Westereng B, Eijsink VGH (2012) Novel enzymes for the degradation of cellulose. Biotechnol. Biofuels

Hu J, Tian D, Renneckar S, Saddler JN (2018) Enzyme mediated nanofibrillation of cellulose by the synergistic actions of an endoglucanase, lytic polysaccharide monooxygenase (LPMO) and xylanase. Sci Rep 8:4–11 . https://doi.org/10.1038/s41598-018-21016-6

Johansen KS (2016) Discovery and industrial applications of lytic polysaccharide mono-oxygenases. Biochem Soc Trans. https://doi.org/10.1042/bst20150204

Kumar S, Stecher G, Tamura K (2016) MEGA7: Molecular Evolutionary Genetics Analysis Version 7.0 for Bigger Datasets. Mol Biol Evol. https://doi.org/10.1093/molbev/msw054

Laskowski RA, MacArthur MW, Moss DS, Thornton JM (2002) PROCHECK: a program to check the stereochemical quality of protein structures. J Appl Crystallogr. https://doi.org/10.1107/s0021889892009944

Liu B, Kognole AA, Wu M, Westereng B, Crowley MF, Kim S, Dimarogona M, Payne CM, Sandgren M (2018a) Structural and molecular dynamics studies of a C1-oxidizing lytic polysaccharide monooxygenase from Heterobasidion irregulare reveal amino acids important for substrate recognition. 285:2225–2242 . https://doi.org/10.1111/febs.14472

Liu B, Krishnaswamyreddy S, Muraleedharan MN, Olson Å, Broberg A, Ståhlberg J, Sandgren M (2018b) Side-by-side biochemical comparison of two lytic polysaccharide monooxygenases from the white-rot fungus Heterobasidion irregulare on their activity against crystalline cellulose and glucomannan. PLoS One. https://doi.org/10.1371/journal.pone.0203430

Morris GM, Huey R, Lindstrom W, Sanner MF, Belew RK, Goodsell DS, Olson AJ (2009) AutoDock4 and AutoDockTools4: Automated Docking with Selective Receptor Flexibility. J Comp Chem. https://doi.org/10.1002/jcc.21256

Müller G, Várnai A, Johansen KS, Eijsink VGH, Horn SJ (2015) Harnessing the potential of LPMO-containing cellulase cocktails poses new demands on processing conditions. Biotechnol Biofuels. https://doi.org/10.1186/s13068-015-0376-y

Nakagawa YS, Kudo M, Loose JSM, Ishikawa T, Totani K, Eijsink VGH, Vaaje-Kolstad G (2015) A small lytic polysaccharide monooxygenase from Streptomyces griseus targeting α- And β-chitin. FEBS J. https://doi.org/10.1111/febs.13203

Pantoom S, Songsiriritthigul C, Suginta W (2008) The effects of the surface-exposed residues on the binding and hydrolytic activities of Vibrio carchariae chitinase A. BMC Biochem 9:1–11 . https://doi.org/10.1186/1471-2091-9-2

Phillips CM, Beeson WT, Cate JH, Marletta MA (2011) Cellobiose dehydrogenase and a copper-dependent polysaccharide monooxygenase potentiate cellulose degradation by Neurospora crassa. ACS Chem Biol. https://doi.org/10.1021/cb200351

Pronk S, Páll S, Schulz R, Larsson P, Bjelkmar P, Apostolov R, Shirts MR, Smith JC, Kasson PM, Van Der Spoel D, Hess B, Lindahl E (2013) GROMACS 4.5: A high-throughput and highly parallel open source molecular simulation toolkit. Bioinformatics. https://doi.org/10.1093/bioinformatics/btt055

Quinlan RJ, Sweeney MD, Lo Leggio L, Otten H, Poulsen J-CN, Johansen KS, Krogh KBRM, Jorgensen CI, Tovborg M, Anthonsen A, Tryfona T, Walter CP, Dupree P, Xu F, Davies GJ, Walton PH (2011) Insights into the oxidative degradation of cellulose by a copper metalloenzyme that exploits biomass components. Proc Natl Acad Sci. https://doi.org/10.1073/pnas.1105776108

Saricks C, Santini D, Wang M (1999) Effects of Fuel Ethanol Use on Fuel-Cycle Energy and

Greenhouse Gas Emissions
Sarkar N, Aikat K (2014) Aspergillus fumigatus NITDGPKA3 provides for increased cellulase production. Int J Chem Eng 2014: . https://doi.org/10.1155/2014/959845
Sievers F, Higgins DG (2014) Clustal omega, accurate alignment of very large numbers of sequences. Methods Mol Biol. https://doi.org/10.1007/978-1-62703-646-7_6
Somerville C, Bauer S, Brininstool G, Facette M, Hamann T, Milne J, Osborne E, Paredez A, Persson S, Raab T, Vorwerk S, Youngs H (2004) Toward a systems approach to understanding plant cell walls. Science (80-.).
Tan TC, Kracher D, Gandini R, Sygmund C, Kittl R, Haltrich D, Hällberg BM, Ludwig R, Divne C (2015) Structural basis for cellobiose dehydrogenase action during oxidative cellulose degradation. Nat Commun. https://doi.org/10.1038/ncomms8542
Trott O, Olson AJ (2010) Software news and update AutoDock Vina: Improving the speed and accuracy of docking with a new scoring function, efficient optimization, and multithreading. J Comput Chem. https://doi.org/10.1002/jcc.21334
Vaaje-Kolstad G, Westereng B, Horn SJ, Liu Z, Zhai H, Sørlie M, Eijsink VGH (2010) An oxidative enzyme boosting the enzymatic conversion of recalcitrant polysaccharides. Science (80-). https://doi.org/10.1126/science.1192231
Väljamäe P, Sild V, Nutt A, Pettersson G, Johansson G (1999) Acid hydrolysis of bacterial cellulose reveals different modes of synergistic action between cellobiohydrolase I and endoglucanase I. Eur J Biochem. https://doi.org/10.1046/j.1432-1327.1999.00853.x
Vermaas J V., Crowley MF, Beckham GT, Payne CM (2015) Effects of lytic polysaccharide monooxygenase oxidation on cellulose structure and binding of oxidized cellulose oligomers to cellulases. J Phys Chem B. https://doi.org/10.1021/acs.jpcb.5b00778
X. Lang, D. G. MacDonald, G. A. Hil (2002) Recycle Bioreactor for Bioethanol Production from Wheat Starch II. Fermentation and Economics. Energy Sources. https://doi.org/10.1080/009083101300058426
Yoswathana (2010) Bioethanol Production from Rice Straw. Energy Res J 1:26–31 . https://doi.org/10.3844/erjsp.2010.26.31
Zhang R, Liu Y, Zhang Y, Feng D, Hou S, Guo W, Niu K, Jiang Y, Han L, Sindhu L, Fang X (2019) Identification of a thermostable fungal lytic polysaccharide monooxygenase and evaluation of its effect on lignocellulosic degradation. Appl Microbiol Biotechnol 103:5739–5750 . https://doi.org/10.1007/s00253-019-09928-3
Zhang Y (2008) I-TASSER server for protein 3D structure prediction. BMC Bioinformatics. https://doi.org/10.1186/1471-2105-9-40
Zhou X, Zhu H (2020) Current understanding of substrate specificity and regioselectivity of LPMOs. Bioresour Bioprocess 7: . https://doi.org/10.1186/s40643-020-0300-6

Figure legends:

Figure 1 In silico analysis of *Af*AA16. (a) Schematic diagram of *Af*AA16; signal peptide: 1-19 amino acids, catalytic domain: 20-189 amino acids, and serine rich domain: 189-289 amino acids. (b) Conserved motif between *Af*AA16 and AA10 C1 oxidising and C1/C4

oxidising LPMOs. (c) Multiple sequence alignment of LPMOs: Conserved sequences are highlighted. The arrow indicates the amino acid responsible for regioselectivity. (d) Electrostatic surface potential of *Af*AA16 model structure at pH6.0, The area sourrounded by the ring represents the catalytic site. (e) Phylogenetic relationship of *Af*AA16 with other AA10LPMOs. A neighbour-joining tree from MEGA showing C1(Bacterial) & C2(Fungal) clades and C2 clade further divided into C2.1(Penicillium & other) & C2.2 (Aspergillus) sub clades.

Figure 2 Model structure and molecular docking of *Af*AA16. (a) Predicted three-dimensional models of the *Af*AA16 showing functional loops LS(orange), L2(blue), L3(green), LC(magenta) loops surrounding the copper active site. (b) Histidine brace (His20, His109) of *Af*AA16 surrounding the copper metal. (c) Amino acids involved in substrate binding: Gln48, Gln181, Ser178, His109, His20, Asn54, Asp50, Tyr252, Glu58

Figure 3 Expression and purification of *Af*AA16. (a) SDS PAGE analysis; lane1. flow through, lane 5 & 6. purified *Af*AA16. (b) Western blot analysis of lane 5 & 6

Figure 4 Enzyme kinetics studies of *Af*AA16 with 2,6-DMP (mean values are plotted). (a) chemical reaction to convert 2,6DMP to 1-coerulignone. (b) Time vs 1-coerulignone concentration plot. (c) LB plot or 1/v vs 1/[s] plot.

Figure 5 Glycosidase activity of *Af*AA16. (a) CMC depolymerisation: estimation of reducing sugar with increasing concentration of *Af*AA16. (b) PASC hydrolysis: relative absorbance at 405 vs *Af*AA16 concentration plot. Results are the mean value of minimum three experiments. The bar represents the standard deviation (SD).

Figure 6 Synergistic effect of *Af*AA16. (a) Hydrolysis of alkali pre-treated rice straw: light-grey bar indicates only cellulase and deep-grey indicates heat inactive *Af*AA16 with cellulase, dark-grey and black bar indicates cellulase along with two different concentration of *Af*AA16. (b) Avicel hydrolysis: reducing sugar estimation. Light-grey bar indicates only cellulase and deep-grey indicates heat inactive *Af*AA16 with cellulase, dark-grey and black bar indicates cellulase along with two different concentration of *Af*AA16. Results are the mean value of minimum three experiments. The bar represents the standard deviation (SD).

Table 1 Enzyme kinetics of *Af*AA16 with 2,6, DMP as a substrate.

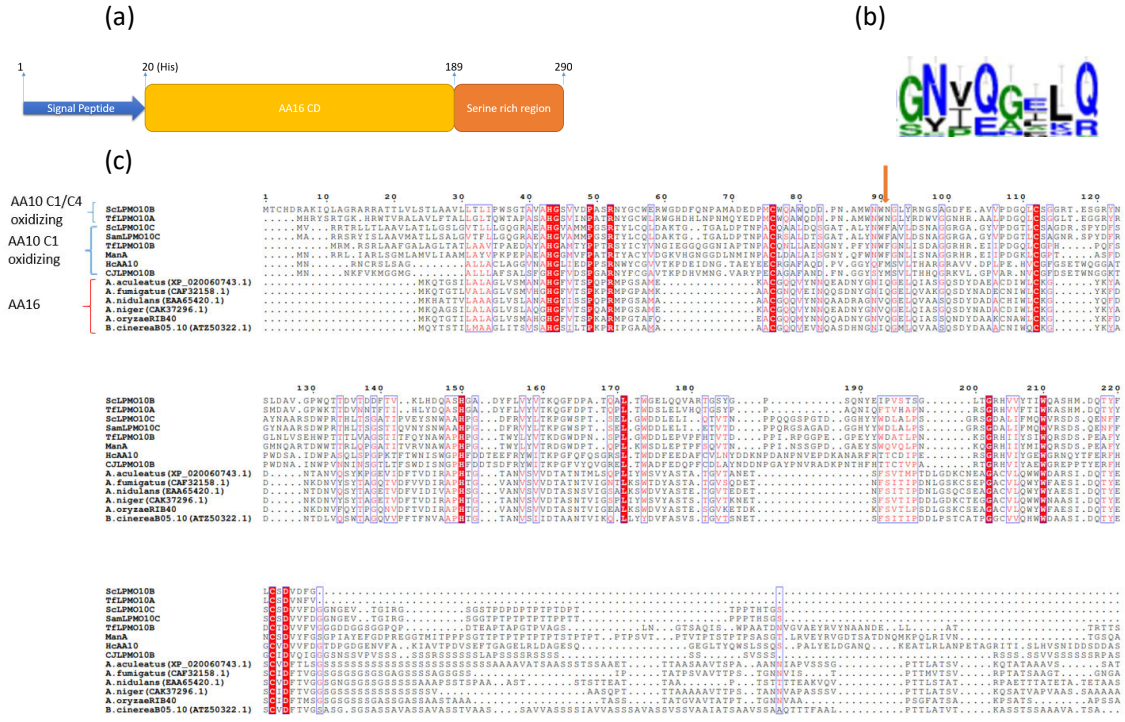
(a)
(b)
1
20 (His)
189
290
Signal Peptide
AA16 CD
Serine rich region
(c)
AA10 C1/C4 oxidizing
AA10 C1 oxidizing
AA16
ScLPM010B
TfLPM010A
ScLPM010C
SamLPM010C
TfLPM010B
ManA
HcAA10
CJLPM010B
A.aculeatus(XP_020060743.1)
A.fumigatus(CAF32158.1)
A.nidulans(EAA65420.1)
A.niger(CAK37296.1)
A.oryzaeRIB40
B.cinereaB05.10(ATZ50322.1)

Figure:1

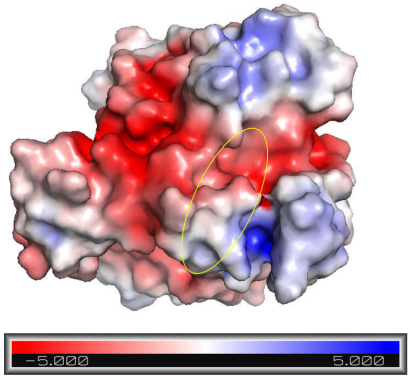

(d)

Figure 1:

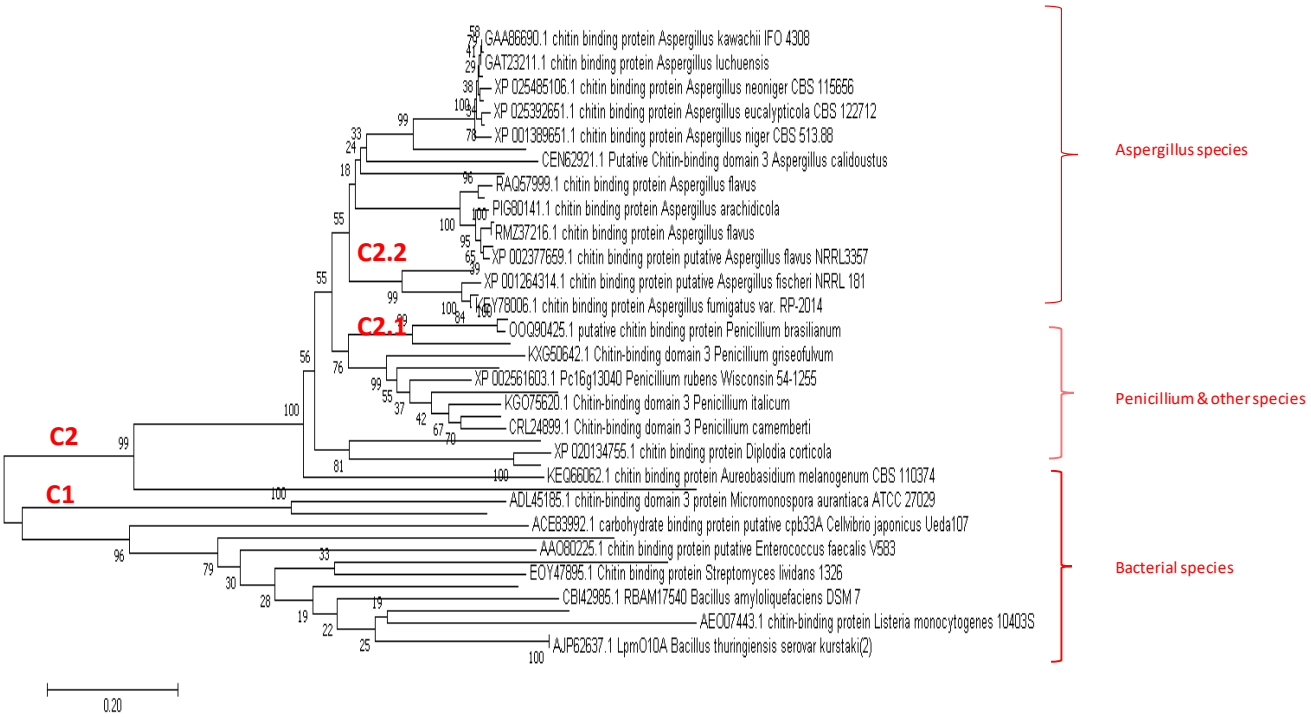
GAA86690.1 chitin binding protein Aspergillus kawachii IFO 4308
GAT23211.1 chitin binding protein Aspergillus luchuensis
XP 025485106.1 chitin binding protein Aspergillus neoniger CBS 115656
XP 025392651.1 chitin binding protein Aspergillus eucalypticola CBS 122712
XP 001389651.1 chitin binding protein Aspergillus niger CBS 513.88
CEN62921.1 Putative Chitin-binding domain 3 Aspergillus calidoustus
RAQ57999.1 chitin binding protein Aspergillus flavus
PIG80141.1 chitin binding protein Aspergillus arachidicola
RMZ37216.1 chitin binding protein Aspergillus flavus
XP 002377659.1 chitin binding protein putative Aspergillus flavus NRRL3357
XP 001264314.1 chitin binding protein putative Aspergillus fischeri NRRL 181
KEY78006.1 chitin binding protein Aspergillus fumigatus var. RP-2014
OOQ90425.1 putative chitin binding protein Penicillium brasilianum
KXG50642.1 Chitin-binding domain 3 Penicillium griseofulvum
XP 002561603.1 Pc16g13040 Penicillium rubens Wisconsin 54-1255
KGO75620.1 Chitin-binding domain 3 Penicillium italicum
CRL24899.1 Chitin-binding domain 3 Penicillium camemberti
XP 020134755.1 chitin binding protein Diplodia corticola
KEQ66062.1 chitin binding protein Aureobasidium melanogenum CBS 110374
ADL45185.1 chitin-binding domain 3 protein Micromonospora aurantiaca ATCC 27029
ACE83992.1 carbohydrate binding protein putative cpb33A Cellvibrio japonicus Ueda107
AAO80225.1 chitin binding protein putative Enterococcus faecalis V583
EOY47895.1 Chitin binding protein Streptomyces lividans 1326
CBI42985.1 RBAM17540 Bacillus amyloliquefaciens DSM 7
AEO07443.1 chitin-binding protein Listeria monocytogenes 10403S
AJP62637.1 LpmO10A Bacillus thuringiensis serovar kurstaki(2)
C2.2
C2.1
C2
C1
Aspergillus species
Penicillium & other species
Bacterial species
0.20

Figure:1 (e)

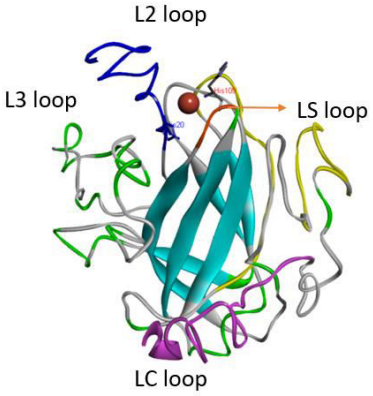

Figure 2 (a)

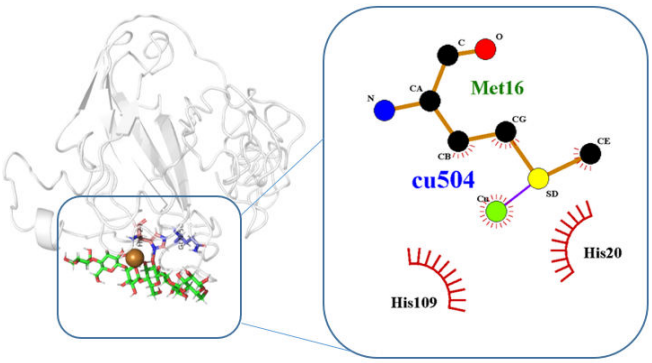
C
O
N
CA
Met16
CG
CE
CB
cu504
SD
Cu
His20
His109

(b)

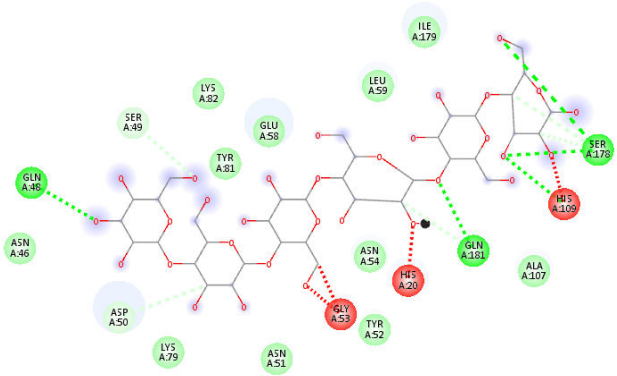
ILE A:179
LEU A:59
LYS A:82
SER A:49
GLU A:58
TYR A:81
SER A:178
GLN A:48
HIS A:109
ASN A:46
ASN A:54
GLN A:181
ALA A:107
HIS A:20
ASP A:50
GLY A:53
TYR A:52
LYS A:79
ASN A:51

(c)

Figure 2:

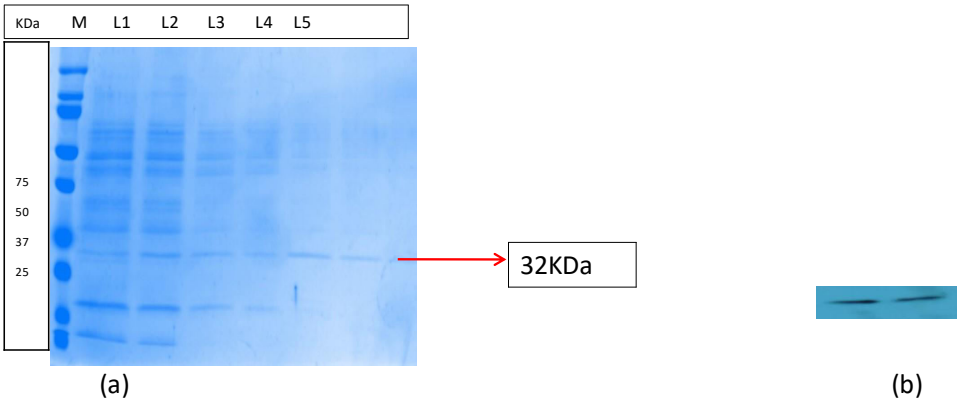

Figure 3:

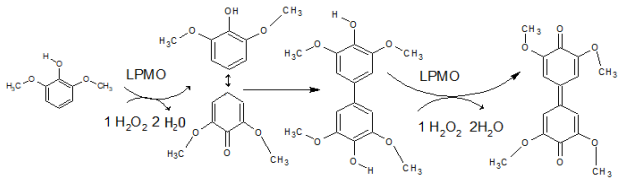
LPMO
1 H2O2 2 H20
LPMO
1 H2O2 2H2O

(a)

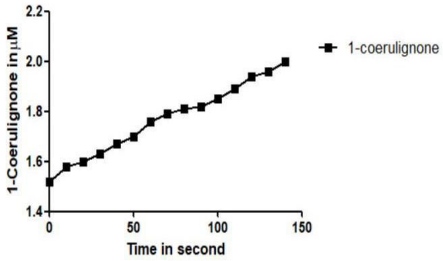
1-Coerulignone in µM
Time in second
1-coerulignone
2.2
2.0
1.8
1.6
1.4
0
50
100
150

(b)

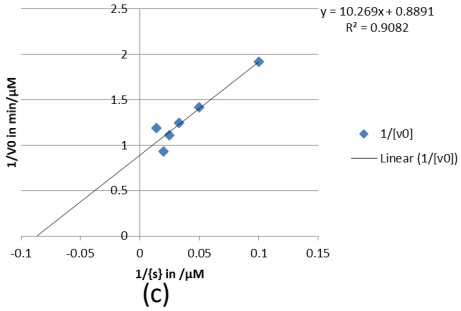
y = 10.269x + 0.8891
R² = 0.9082
1/V0 in min/µM
1/{s} in /µM
1/[v0]
Linear (1/[v0])
2.5
2
1.5
1
0.5
0
-0.1
-0.05
0
0.05
0.1
0.15

(c)

Figure 4

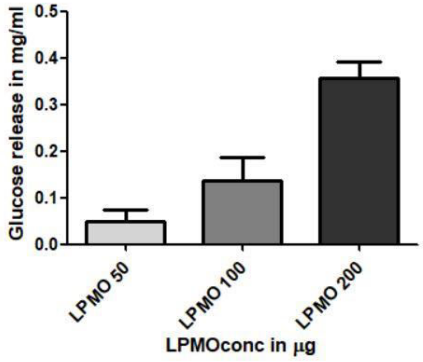
Glucose release in mg/ml
0.5
0.4
0.3
0.2
0.1
0.0
LPMO 50
LPMO 100
LPMO 200
LPMOconc in µg

(a)

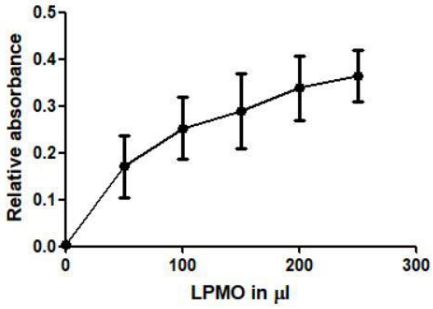
Relative absorbance
0.5
0.4
0.3
0.2
0.1
0.0
0
100
200
300
LPMO in µl

(b)

Figure 5

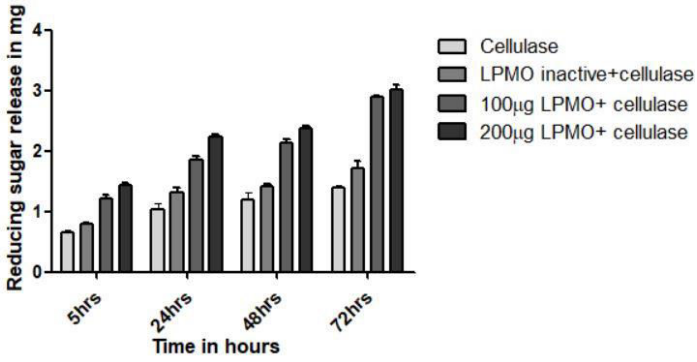
Reducing sugar release in mg
4
3
2
1
0
5hrs
24hrs
48hrs
72hrs
Time in hours
Cellulase
LPMO inactive+cellulase
100µg LPMO+ cellulase
200µg LPMO+ cellulase

(a)

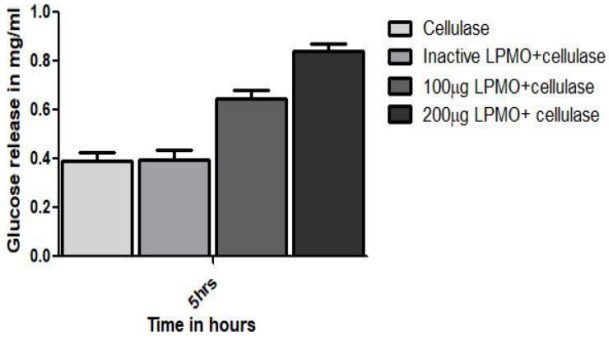
Glucose release in mg/ml
1.0
0.8
0.6
0.4
0.2
0.0
5hrs
Time in hours
Cellulase
Inactive LPMO+cellulase
100µg LPMO+cellulase
200µg LPMO+ cellulase

(b)

Figure 6

Kinetic parameters	values
V_{max} in µM/min	1.1086
K_m in µM	11.23
Specific activity in U/g	37.43
Kcat in /min	0.642

Table 1

Title: Investigation the biomass conversion efficiency, biochemical characterisation and structural insights of the newly isolated AA16 family of Lytic Polysaccharide Monooxygenase (LPMO) from *Aspergillus fumigatus*.

Musaddique Hossain, Subba Reddy Dodda, Bishwajit Singh Kapoor, Kaustav Aikat and Sudit S. Mukhopadhyay*

Department of Biotechnology, National Institute of Technology Durgapur-713209, West Bengal, India
*Corresponding author: suditmukhopadhy@yahoo.com

Supplementary figures;

>AFAA16_LPMO.reverse_18217-2_P3515,Trimmed Sequence(844 bp)
ATGTAGCTGAGCTGCTCCTCAGCAGTGCCGCTGGTGGGGAAAGATGTGGAG
GAGCCAGCGCCATTACCGGTGCCAGCGGCCGAGGTGGCAGTCGGTCTCACG
CTGGTGACCATAGTGGTAGGCGTGGAGATCACGTTGTTTCCGGTGCTGGGA
GTGGTAACAGCAACGCTGGGAGTAGCGGTCGGAATCGAAAAGCCAGAACCA
GCGCTGGAGCTGGAGCCAGCGCCGGAGCCAGAGCCGGAGCCGGAGCCGGA
GCCGCCAACAGTGAAGTCAATGCAGGACTCGTAGGTCTGGTCGATCGACTC
GGCGAACCAGTACCATTGGAGGACACAAGCACCGGGCTCGGAGCACTTGCT
GCCCAGGTTGTCGGGGATGGTGATGCTGAAGTTGGTCTCATCCTGGGAGAC
ACCGGTGGCGGTCGAGGCGTAGTCGGTCCAGGACTTGAGGGTATTGCCAAT
CACCGTGTTGGTAGCGGTGTCAACGACGGAGACGTTGGCCACACCGGTGTG
AGGCGCACGGATGTCAACCACGAAGTCGACGGTCTGGCCGGCGGTGTAGGA
GTAGACGTTGTCCTTGTTGTCGTCAAACTTGTAACCCTTGCAGAGCCAGATG
TTACACTCGTCGGCGTTGTAGTCGCTCTGGCCCTTGGCTACCTGAAGC
TCACCCTGGATGTTGCCGTAGTTGTCGGACTGCTGGTTGATCTCCACCTGGT
TACCGCAGGCAGCCTTCATAGCCGGGCCGGGCATACGGGGCTTGGGGAGA
GGTGACAAAACCGTGACCGTGGACCATGGAGACCAGGCCGGCGAGGGCGA
CGAGAGTGCCGGTTTGCTTCATGAATTCAGCT

Nucleotide sequence of the gene *Af*AA16.

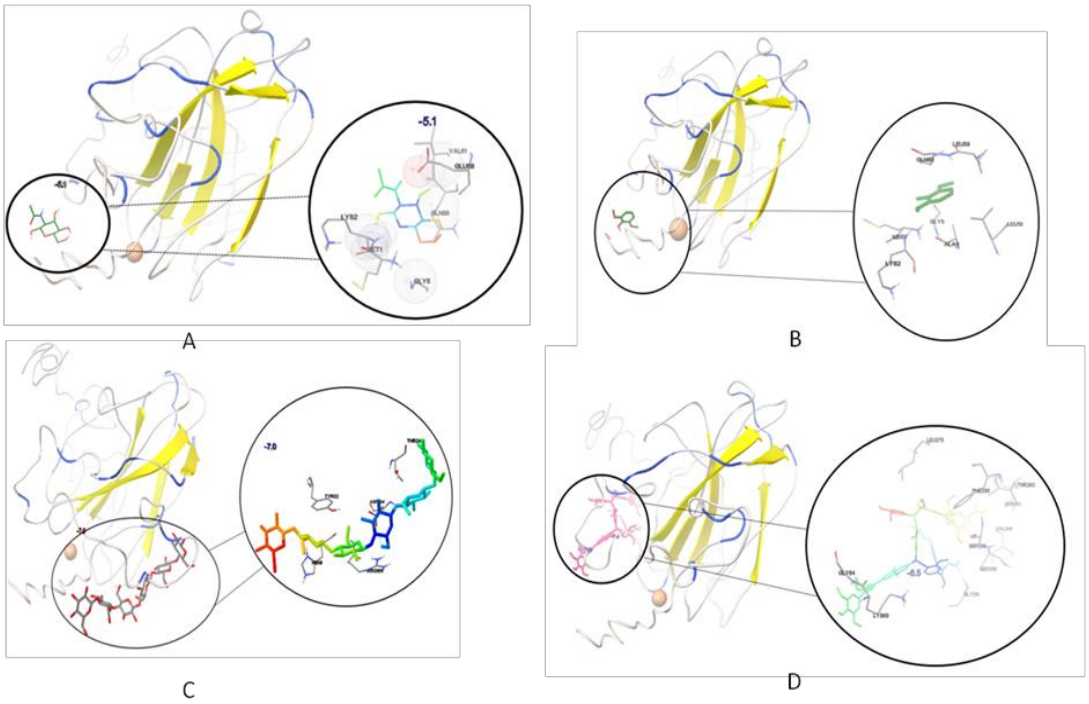

Figure 1:

Substrate specificity analysis by molecular docking: A) chitin binding in the cavity near to copper catalytic center and Met1, Lys2, Gly5, Gln60, Glu60 amino acids are near to the chitin. B) 2,6 DMP a synthetic substrate binding as like natural substrate. C) cellohexose binding in the L2 Loop surface near to the copper catalytic canter, amino acids Thr24, Tyr52, Asp104, and Arg106 are binding to the cellulose. D) Aromatic compound lignin binding to the serine-rich C terminal domain. Amino acids Gly64, Lys63, Ser208, Ser209, Ser251, Phe265 are binding to the lignin.

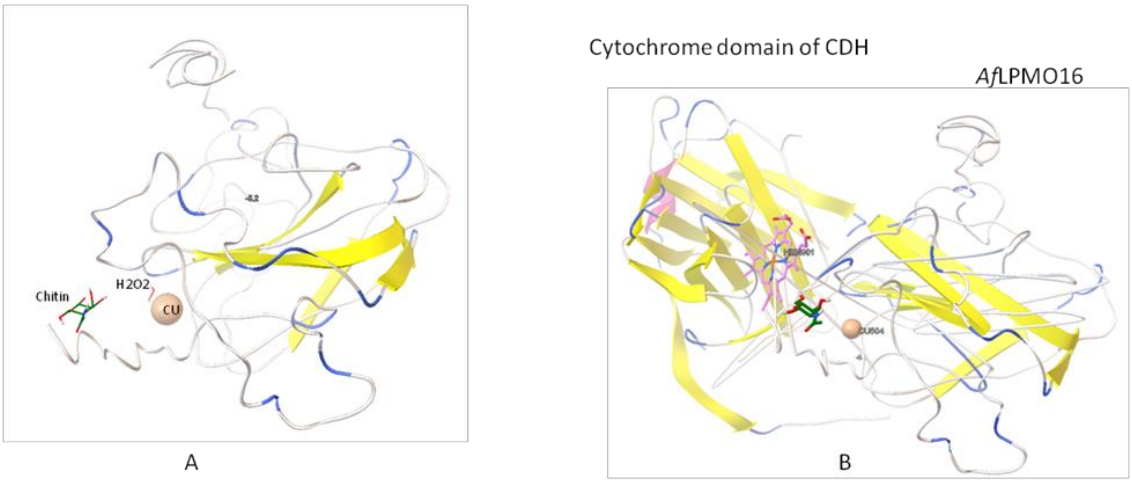

Figure:2

Co-Substrate specificity of *Af*AA16 by Molecular docking: A) H_2O_2 *Af*AA16- chitin B) Cytochrome domain of CDH *Af*AA16- chitin.

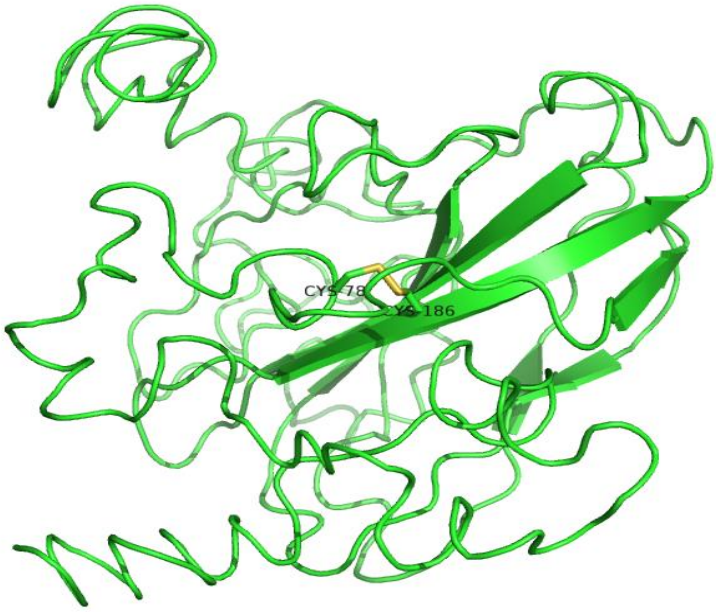

Supplementary figure: 3 *Af*AA16 showing single disulphide bond formed by the Cys78, Cys186 near to the copper catalytic centre.